Water-Catalyzed Dehalogenation Reactions of the Isomer of CBr_4 and Its Reaction Products and a Comparison to Analogous Reactions of the Isomers of Di- and Trihalomethanes

Cunyuan Zhao,[a, b] Xufeng Lin,[a] Wai Ming Kwok,[a] Xiangguo Guan,[a] Yong Du,[a] Dongqi Wang,[a] Kam Fa Hung,[a] and David Lee Phillips*[a]

Abstract: A combined experimental and theoretical study of the UV photolysis of a typical tetrahalomethane, CBr_4, in water and acetonitrile/water was performed. Ultraviolet photolysis of low concentrations of CBr_4 in water mostly leads to the production of four HBr leaving groups and CO_2. Picosecond time-resolved resonance Raman (Ps-TR^3) experiments and ab initio calculations indicate that water-catalyzed O–H insertion/HBr elimination of the isomer of CBr_4 and subsequent reactions of its products lead to the formation of these products. The UV photolyses of di-, tri-, and tetrahalomethanes at low concentrations in water-solvated environments are compared to one another. This comparison enables a general reaction scheme to be deduced that can account for the different products produced by UV photolysis of low concentrations of di-, tri-, and tetrahalomethanes in water. The fate of the (halo)formaldehyde intermediate in the chemical reaction mechanism is the key to determining how many strong acid leaving groups are produced and which carbon atom final product is likely formed by UV photolysis of a polyhalomethane at low concentrations in a water-solvated environment.

Keywords: ab initio calculations · dehalogenation · elimination · reaction mechanisms · water chemistry

Introduction

Polyhalomethanes such as CH_2I_2, CH_2BrI, $CHBr_3$, CCl_4, $CFCl_3$, and others have been observed in the natural environment from natural and/or anthropogenic sources, and they are important sources of reactive halogens that have been linked to ozone depletion in both the troposphere and the stratosphere.[1–11] Both gas- and condensed phase photochemistry and chemistry are important for accurately describing reactions in the natural environment.[1–3] Thus, halogen activation processes in the natural environment have recently been an area of active investigation.[12–22] In addition, there is increasing interest in how polyhalomethanes such as CH_2I_2 facilitate the formation of iodine aerosols in the atmosphere.[23] Polyhalomethanes have also been used to study photochemical water treatment processes, to better understand the dehalogenation and decomposition of halogenated organic compounds, and to potentially help design and improve photocatalysts for water treatment.[24–27]

Ultraviolet photolysis with the 253.7 nm line of a Hg lamp of low concentrations ($<10^{-6}$ M) of trihalomethanes (e.g., $CHBr_3$, $CHBr_2Cl$, and $CHCl_2Br$) in water was observed to lead to complete conversion of the halogens into their halide ions (bromide and/or chloride) with similar photoquantum yields of around 0.43.[24] We recently used a combination of photochemical experiments and theoretical calculations to help elucidate the reaction mechanism for photochemical conversion of low concentrations of $CHBr_3$ in water to three bromide ions.[28,29] Ultraviolet excitation of $CHBr_3$ (9×10^{-5} M) in water gave almost complete conversion to three HBr leaving groups and CO (major product) and HCOOH (minor product).[29] Picosecond time-resolved resonance Raman (ps-TR^3) experiments and ab initio calcu-

[a] Prof. C. Zhao, X. Lin, W. M. Kwok, X. Guan, Y. Du, D. Wang, K. F. Hung, Prof. D. L. Phillips
Department of Chemistry
The University of Hong Kong
Pokfulam Road, Hong Kong (P. R. China)
Fax: (+852) 2857-1586
E-mail: phillips@hkucc.hku.hk

[b] Prof. C. Zhao
School of Chemistry & Chemical Engineering
Sun Yat-Sen University
Guangzhou 510275 (P. R. China)

Supporting information for this article is available on the WWW under http://www.chemeurj.org/ or from the author.

 DOI: 10.1002/chem.200400695

lations indicate that the water-catalyzed O–H insertion/HBr elimination reaction of isobromoform and subsequent reactions of its products are responsible for the formation of the final products observed after UV photolysis of $CHBr_3$ in water.[29] Ultraviolet photolysis of low concentrations of CH_2I_2 in water led to production of methanediol ($CH_2(OH)_2$) and two HI leaving groups as products.[30] Ps-TR^3 experiments and ab initio calculations indicate that water-catalyzed O–H insertion/HI elimination of isodiiodomethane and subsequent reactions of its products are responsible for the formation of methanediol and two HI leaving groups.[30] We note that UV photolysis of dihalomethanes (e.g., CH_2I_2) and trihalomethanes (e.g., $CHBr_3$) led to the formation of different products from the carbon atom of the polyhalomethane. Thus, it is not clear what products will be formed from decomposition of tetrahalomethanes such as CBr_4, CCl_4, and $CFCl_3$.

Here we present a combined experimental and theoretical investigation of the UV photolysis of a typical tetrahaloethane, CBr_4, in water and acetonitrile/water to elucidate what products are formed and the reaction mechanism responsible for their production. We found that UV photolysis of low concentrations of CBr_4 in water leads mainly to formation of four HBr leaving groups and CO_2. Ps-TR^3 experiments and ab initio calculations indicate that water-catalyzed O–H insertion/HBr elimination of the isomer of CBr_4 and subsequent reactions of its products are responsible for the formation of these products. We compare and contrast the UV photolysis of di-, tri-, and tetrahalomethanes at low concentrations in water-solvated environments. A general reaction scheme is presented that can account for the different products produced by UV photolysis of low concentrations of di-, tri-, and tetrahalomethanes in water. The potential implications of these results for the photochemistry of polyhalomethanes in the natural environment are briefly discussed.

Experimental and Computational Details

Photochemical experiments: Sample solutions were prepared from commercially available CBr_4, $^{13}CBr_4$, D_2O (99.9% D), and deionized water. Samples of about 7×10^{-5} M CBr_4 were placed in a glass holder (10 cm path length) with quartz windows. The sample solution was excited with about 1 mJ of 266 nm light from an unfocused laser beam from the fourth harmonic of an Nd:YAG laser. The absorption spectra of the photolyzed samples were acquired by using a 1-cm UV grade cell and a Perkin Elmer Lambda 19 UV/Vis spectrometer. The pH of the photolyzed samples was measured with a THERMO Orion 420A pH meter equipped with a 8102BN combination pH electrode that was calibrated with pH 7.00 and 4.01 buffer solutions. ^{13}C NMR and ^1H NMR spectra were acquired with a Bruker Avance 400 DPX spectrometer and air-tight $\varnothing = 5$ mm sample tubes at room temperature. The $^{13}CBr_4$ concentration was about 1.0 mM in D_2O. IR spectra were obtained on a FTS 165 spectrometer after transfer of the gas evolved in the photolysis experiments to a gas sample holder.

Picosecond time-resolved resonance Raman experiments: A commercial femtosecond mode-locked Ti:sapphire regenerative amplifier laser was used for the experiments. The output from the laser (800 nm, 1 ps, 1 kHz) was frequency-doubled and -tripled by potassium dihydrogenphosphate (KDP) crystals to generate the 400 nm probe and 267 nm pump wavelengths used in the experiments. Fluorescence depletion of *trans*-stilbene was employed to find the time-zero delay between the pump and probe laser beams. The optical delay between the pump and probe beams was varied to a position where the depletion of the stilbene fluorescence was halfway to the maximum fluorescence by the probe laser. The uncertainty of the time-zero measurement was estimated to be ± 0.5 ps, and a typical cross-correlation time was determined to be about 1.5 ps (FWHM). The pump and probe laser beams with magic-angle polarization were lightly focused onto a flowing liquid jet of sample about 500 μm thick. Typical pulse energies and spot sizes at the sample were 15 μJ and 250 μm for the pump beam and 8 μJ and 150 μm for the probe beam. A backscattering geometry was employed to excite the sample and to collect the Raman-scattered light. The Raman light was imaged through the entrance slit of a 0.5 m spectrograph whose grating dispersed the light onto a liquid-nitrogen-cooled CCD detector at the exit port of the spectrograph.

Each ps-TR^3 spectrum was obtained by subtraction of scaled probe-before-pump and scaled net solvent measurements from a pump-probe spectrum so that contributions from parent CBr_4 Raman bands and residual solvent Raman bands, respectively, were deleted. The known Raman shifts of the solvent Raman bands were used to calibrate the spectra with an uncertainty of about $\pm 5\ cm^{-1}$ in absolute frequency. Commercially available CBr_4 (99%), deionized water, and spectroscopic-grade acetonitrile were used to prepare half-liter CBr_4 sample solutions with different amounts of water (trace amounts and 5 vol%). The samples showed less than a few percent decomposition during the experiments, as deduced from UV/Vis spectra obtained before and after the ps-TR^3 experiments.

Ab initio calculations: Second-order Møller–Plesset perturbation theory (MP2) with frozen-core approximation was used to investigate six types of water-assisted reactions [Eqs. (1)–(6)].

$$(Br_2CBr{-}Br) + n\,H_2O \rightarrow CBr_3(OH) + HBr + (n{-}1)\,H_2O \ (n = 1,2,3) \quad (1)$$

$$CBr_3(OH) + n\,H_2O \rightarrow CBr_2O + HBr + n\,H_2O \ (n = 0, 1, 2, 3) \quad (2)$$

$$CBr_2O + n\,H_2O \rightarrow BrCOOH + HBr + (n{-}1)\,H_2O \ (n = 1, 2, 3, 4) \quad (3)$$

$$CBr_2O + n\,H_2O \rightarrow CBr_2(OH)_2 + (n{-}1)H_2O \ (n = 1, 2) \quad (4)$$

$$CBr_2(OH)_2 + n\,H_2O \rightarrow BrCOOH + HBr + n\,H_2O \ (n = 0, 1, 2, 3) \quad (5)$$

$$BrCOOH + n\,H_2O \rightarrow CO_2 + HBr + n\,H_2O \ (n = 0, 1, 2) \quad (6)$$

Geometry optimization and frequency calculations were accomplished with the 6-31G* basis set for the C, H, O, and Br atoms. All calculations used the Gaussian 98 program suite.[31] The Cartesian coordinates, total energies, and selected output from the calculations for all of the calculated structures are provided in the Supporting Information. Intrinsic reaction coordinate (IRC) computations[32] were done to confirm that the transition state connected the appropriate reactants and products for all reactions. A summary of the IRC computations, including energies, reaction coordinate, and the Cartesian or internal coordinates of the above six types of reactions with maximum number of water molecules are also included in the Supporting Information.

Results and Discussion

Photochemistry: Figure 1a presents UV/Vis absorption spectra acquired following varying times of 266 nm laser photolysis of a 7×10^{-5} M CBr_4 sample in water. The absorption band due to CBr_4 in the 220–240 nm region decreases in intensity, whereas that for the Br^- ion in the 200 nm region increases in intensity with increasing photolysis time. A clear isosbestic point at about 225 nm indicates that Br^-

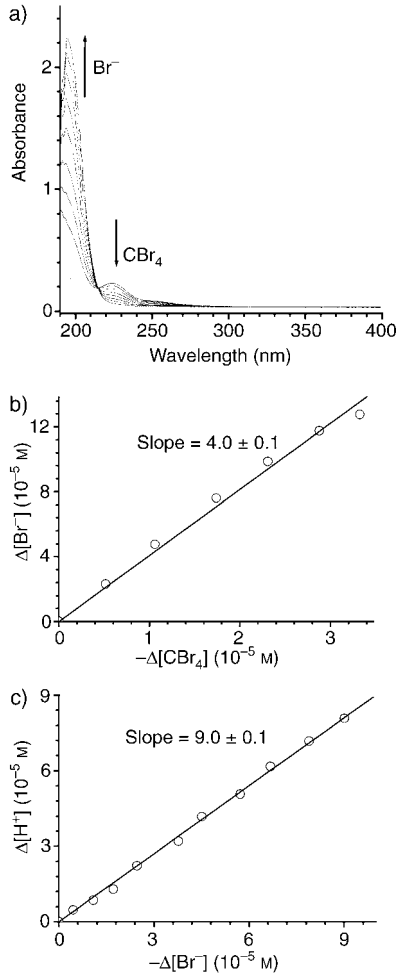

Figure 1. a) Absorption spectra obtained after varying times of photolysis of a 7×10^{-5} M CBr_4 sample in water. b) Plots of $[Br^-]$ versus $-[CBr_4]$ obtained from the spectra in a). c) Plots of the changes in $[H^+]$ determined from pH measurements versus changes in $[Br^-]$ determined from the spectra in a).

is directly formed from the parent CBr_4 molecule. The pH of the sample solution was measured for each of the UV/Vis spectra shown in Figure 1a. The measured molar extinction coefficients for CBr_4 and Br^- were employed to determine the concentrations of these species for each photolysis time from the UV/Vis spectra of Figure 1a. Plots of $\Delta[Br^-]$ versus $-\Delta[CBr_4]$ (Figure 1b) during the photochemistry experiments display a linear relationship with a slope of about 4. This indicates that UV photolysis of low concentrations of CBr_4 in water produced four Br^- ions. Plots of $\Delta[H^+]$ determined from the pH measurements versus $\Delta[Br^-]$ (Figure 1c) show a linear correlation with a slope of about 0.9, which is close to 1 and suggests that each Br^- ion is accompanied by formation of an H^+ ion, similar to previous photochemical results for $CHBr_3$.[28,29] The UV/Vis and pH photochemical data in Figure 1 suggest that UV photolysis of low concentrations of CBr_4 releases four H^+ and four Br^- ions (likely from four HBr leaving groups that immediately dissociate into H^+ and Br^- ions in water).

To learn more about what happens to the carbon atom from the CBr_4 parent molecule after 266 nm photolysis, we next employed a ^{13}C-labeled sample of CBr_4 in the photochemistry experiments. We then repeated the 266 nm photolysis experiments and acquired ^{13}C NMR spectra before, during, and after complete photolysis of $^{13}CBr_4$ in a D_2O (99%)/CD_3CN (1%) (Figure 2a). The small amount of

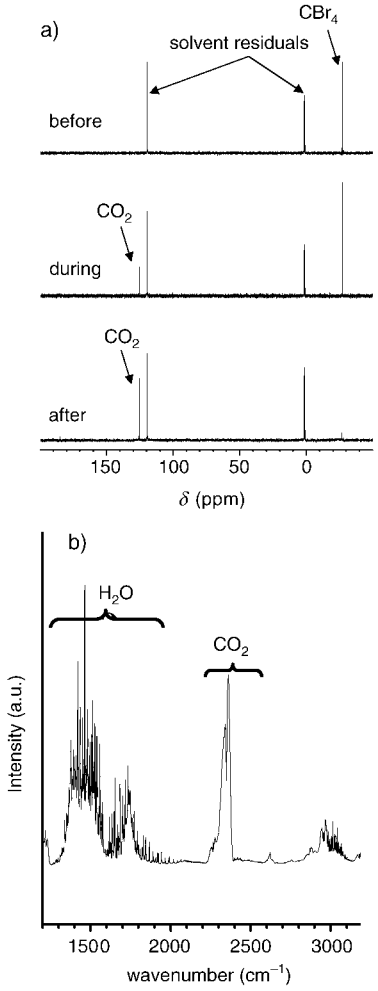

Figure 2. a) 266 nm photolysis experiments and ^{13}C NMR spectra acquired before, during, and after complete photolysis of $^{13}CBr_4$ in D_2O (99%)/CD_3CN (1%). The parent $^{13}CBr_4$ band appears at about -50 ppm in the ^{13}C NMR spectra. Photolysis converts $^{13}CBr_4$ to a photoproduct with a band at 125 ppm, assigned to CO_2. b) IR spectrum of the gas obtained during the 266 nm photolysis of CBr_4 in water. The bands at 2340 and 2360 cm^{-1} are assigned to CO_2.

CD_3CN in the solvent system provides convenient reference bands during the experiments. Similar results were obtained when photolysis was performed in D_2O without CD_3CN. The parent $^{13}CBr_4$ band at about -50 ppm decreases with increasing photolysis time, while a new band for a photoproduct appears at about 125 ppm. This band is assigned to CO_2, and this was confirmed by comparison to an authentic sample of CO_2. The gas evolved during the NMR photo-

chemical experiments was then collected and placed in a gas IR sample cell and its IR spectrum recorded (Figure 2b). The two bands at 2340 and 2360 cm^{-1} are characteristic of CO_2 gas, and this further confirms the NMR assignment of CO_2 being produced from the photolysis.

The above photochemical results suggest that UV photolysis of low concentrations of CBr_4 in water leads to the following overall reaction giving its major reaction products [Eq. (7)].

$$CBr_4 + h\nu + n\,H_2O \rightarrow CO_2 + 4\,HBr + (n-2)\,H_2O \qquad (7)$$

The experimental results in Figures 1 and 2 also suggest that this reaction can convert almost all of the parent CBr_4 at low concentration to mainly CO_2 and 4 HBr and little if any other products. Previous photochemical experiments on trihalomethanes such as $CHBr_3$, $CHBr_2Cl$, and $CHCl_2Br$ found that UV excitation (253.7 nm light from a Hg lamp) at low concentrations ($<10^{-6}$ M) in water led to complete conversion of the organic halogen of the polyhalomethanes to halide ions (Br^- and/or Cl^-) with a similar photoquantum yield of 0.43.[24] Our present results for CBr_4 and the dihalomethane CH_2I_2 at relatively low concentrations[30] are consistent with the results for trihalomethanes, that is, conversion of organic halogens to halide ions with an appreciable photoquantum yield. This suggests that it is probably fairly common for UV excitation of many polyhalomethanes at low concentrations in water to lead to almost quantitative conversion to halide ions.

What species produced by the UV photolysis of CBr_4 in aqueous solution can react efficiently to form the CO_2 and 4 HBr observed as products in the photochemical experiments? We recently observed that photolysis of polyhalomethanes such as CH_2I_2 and $CHBr_3$ in aqueous environments can form appreciable amounts of isopolyhalomethanes.[28–30,33] In the case of $CHBr_3$ we were able to directly observe the O–H insertion reaction of the isobromoform species with water to produce a $CHBr_2OH$ product that undergoes further water-catalyzed decomposition reactions.[28,29] In the next section, we present picosecond time-resolved resonance Raman experiments performed to examine what photoproducts are produced shortly after photolysis of CBr_4 in the presence of water and whether they can react with water.

Picosecond time-resolved resonance Raman (ps-TR^3) spectroscopy: Figure 3 shows selected ps-TR^3 spectra acquired for the initial photoproducts after 267 nm photolysis of CBr_4 in acetonitrile containing traces of water (ca. 0.1 %) and acetonitrile/water (95/5). Inspection of the spectra in Figure 3 reveals that a photoproduct is formed within several picoseconds that has prominent Raman bands at about 280 and 828 cm^{-1} which correspond to vibrational bands for the nominal Br-Br-C-Br symmetric stretching fundamental (ν_3) and the nominal C–Br stretching fundamental (ν_1) for the isomer of CBr_4 (denoted hereafter as isotetrabromomethane). This behavior is very similar to previous ps-TR^3

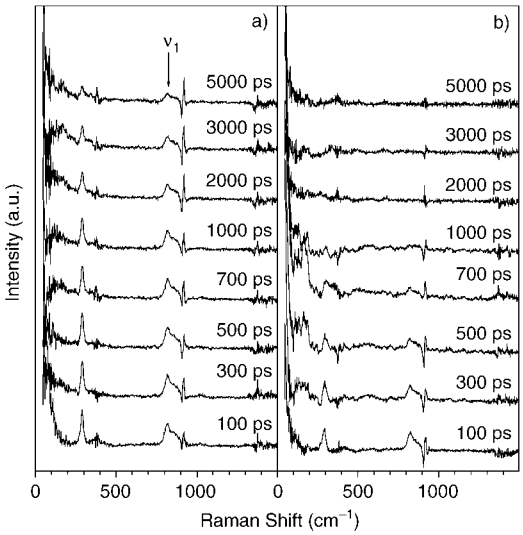

Figure 3. Stokes ps-TR^3 spectra obtained following 267 nm photolysis of CBr_4 in acetonitrile/water at a probe excitation wavelength of 400 nm. Spectra in a) and b) were obtained with a trace and 5 % water, respectively.

spectra observed for formation of other related isopolyhalomethanes such as isobromoform and isodiiodomethane following UV photolysis in acetonitrile and acetonitrile/water.[28–30,33] The prominent ν_1 C–Br stretching fundamental band in the spectra is in excellent agreement with the observation of the same band for isotetrabromomethane previously observed by ns-TR^3 spectroscopy in cyclohexane and clearly identifies this species, since the C–Br stretch shifts significantly in other likely photoproducts such as CBr_4^+, CBr_3 radical, and CBr_3^+.[34] The different probe wavelength (400 nm) and/or polar solvents used in the ps-TR^3 experiments reported here probably account for why the ν_3 mode is more clearly observed in these spectra than in the previous ns-TR^3 spectra obtained with a probe wavelength of 436 nm in cyclohexane.[34]

The Raman band at about 828 cm^{-1}, assigned to the fundamental nominal C–Br stretch mode (ν_1), was integrated at different time delays so as to inspect the kinetics of the growth and decay of isotetrabromomethane. Figure 4 show plots of the relative integrated areas of the ν_1 Raman band from 100 to 6000 ps in acetonitrile and water/acetonitrile. They fit to a simple function [dotted lines in Figure 4 represent these fits; Eq. (a)], where $I(t)$ is the relative integrated area of the ν_1 Raman band, t the time, t_1 the decay time constant of the ν_1 Raman band, t_2 the growth time constant of the ν_1 Raman band, and A and B are constants.

$$I(t) = Ae^{-t/t_1} - Be^{-t/t_2} \qquad (a)$$

The fits to the data in Figure 4 found that the isotetrabromomethane photoproduct had time constants t_1 of 2540 and 587 ps for its decay in acetonitrile with water concentrations of trace amounts and 5 %, respectively. The isotetrabromo-

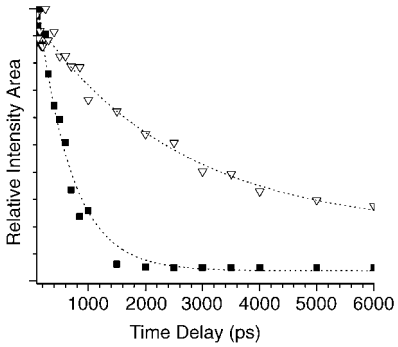

Figure 4. Plots of the relative integrated area of the ν_1 Raman band of isotetrabromomethane at different delay times obtained in acetonitrile with trace amounts of water (▽) and 5% water/95% acetonitrile (■). The dotted lines represent least-squares fits to the data (see text for details).

methane Raman bands decay with a lifetime that decreases substantially as the water concentration increases, and this suggests isotetrabromomethane may react with water. This behavior of isotetrabromomethane in the presence of increasing amounts of water is very similar to the much faster decay of isobromoform and isodiiodomethane as the amount of water in the solvent increases.[28–30,33] In the case of isobromoform, the O–H insertion reaction to produce a $CHBr_2OH$ as product could be directly observed in the ps-TR^3 experiments.[28,29] Therefore, one can expect isotetrabromomethane to react with water by an analogous reaction, and this was examined by ab initio calculations.

Ab initio calculations for O–H insertion and/or HBr elimination reactions associated with the decomposition of isotetrabromomethane: Figures 5–10 show optimized geome-

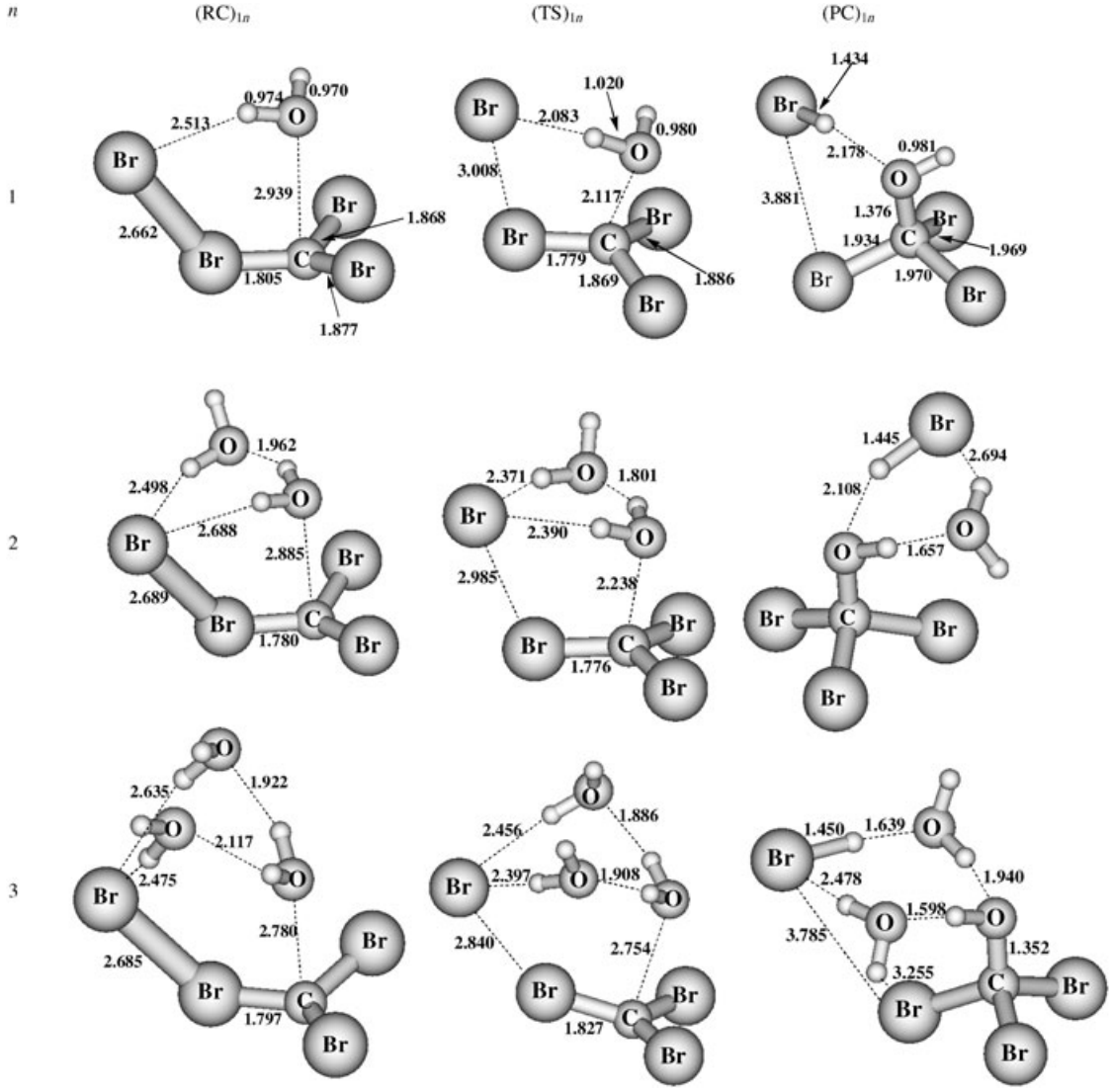

Figure 5. Optimized geometries for the reactant complexes, transition states, and product complexes obtained from MP2/6-31G* calculations on the isotetrabromomethane reactions $(Br_2CBr{-}Br) + n\,H_2O \rightarrow CBr_3(OH) + HBr + (n-1)\,H_2O$ ($n = 1, 2, 3$) with $(RC)_{1n}$, $(TS)_{1n}$,and $(PC)_{1n}$, where $n = 1, 2, 3$, respectively.

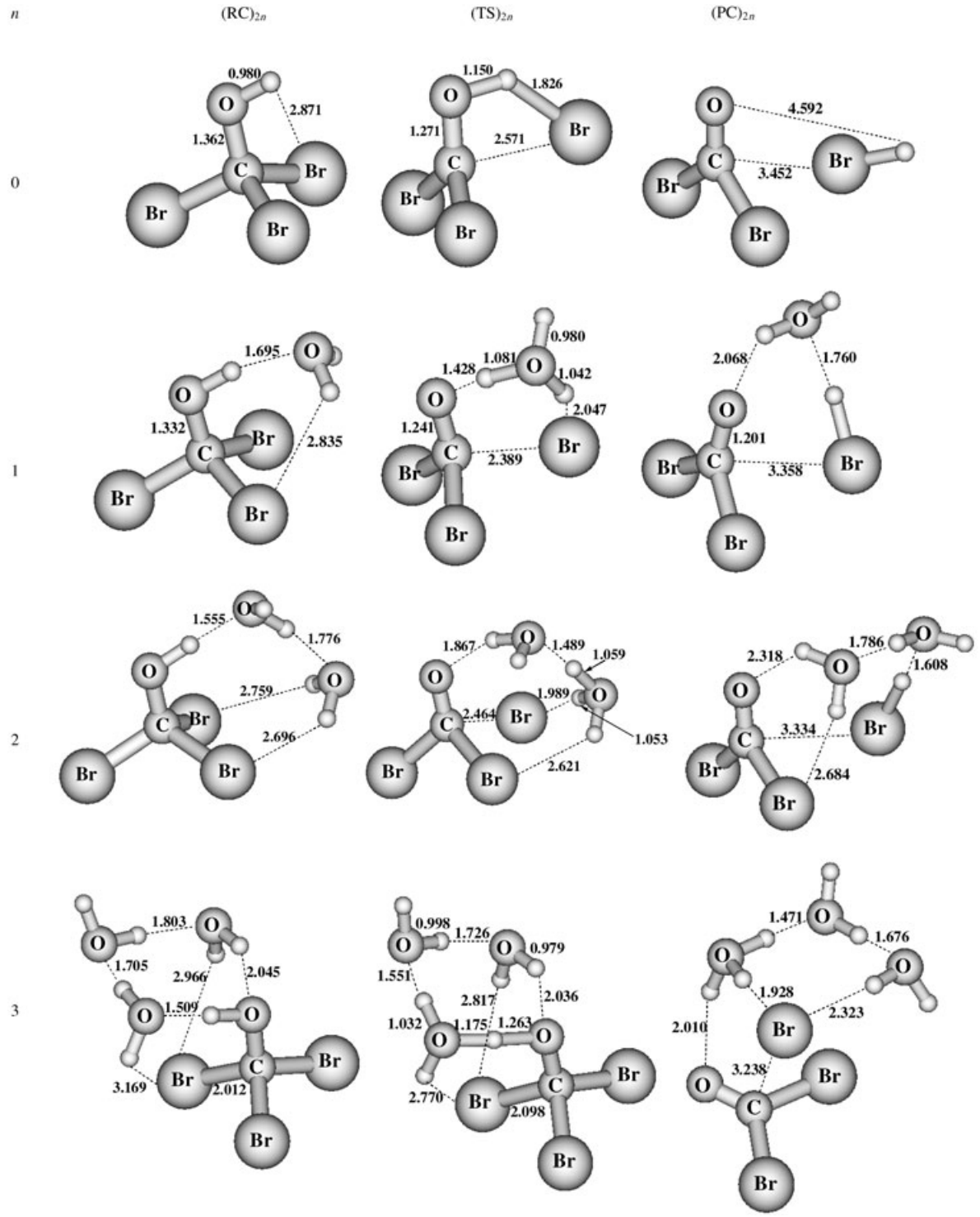

Figure 6. Optimized geometries for the reactant complexes, transition states, and product complexes obtained from MP2/6-31G* calculations for the $CBr_3(OH)+n\,H_2O \rightarrow CBr_2O+HBr+n\,H_2O$ ($n=0$, 1, 2, 3) reactions with $(RC)_{2n}$, $(TS)_{2n}$, and $(PC)_{2n}$,where $n=0$, 1, 2, 3, respectively.

tries with selected bond lengths, and Figure 11 shows schematic diagrams of the relative free energy (298.15 K) profiles (in kcal mol^{-1}) obtained from MP2/6-31G* calculations on reactant complexes, transition states, product complexes, and products for the reactions of isotetrabromomethane [Eq. (1)] and the decomposition or O–H insertion reactions [Eq. (2)–(6)].

Figure 11 shows that the barriers to reaction (e.g., from the reactant complexes to their respective transition states) become substantially smaller as the number of H_2O mole-

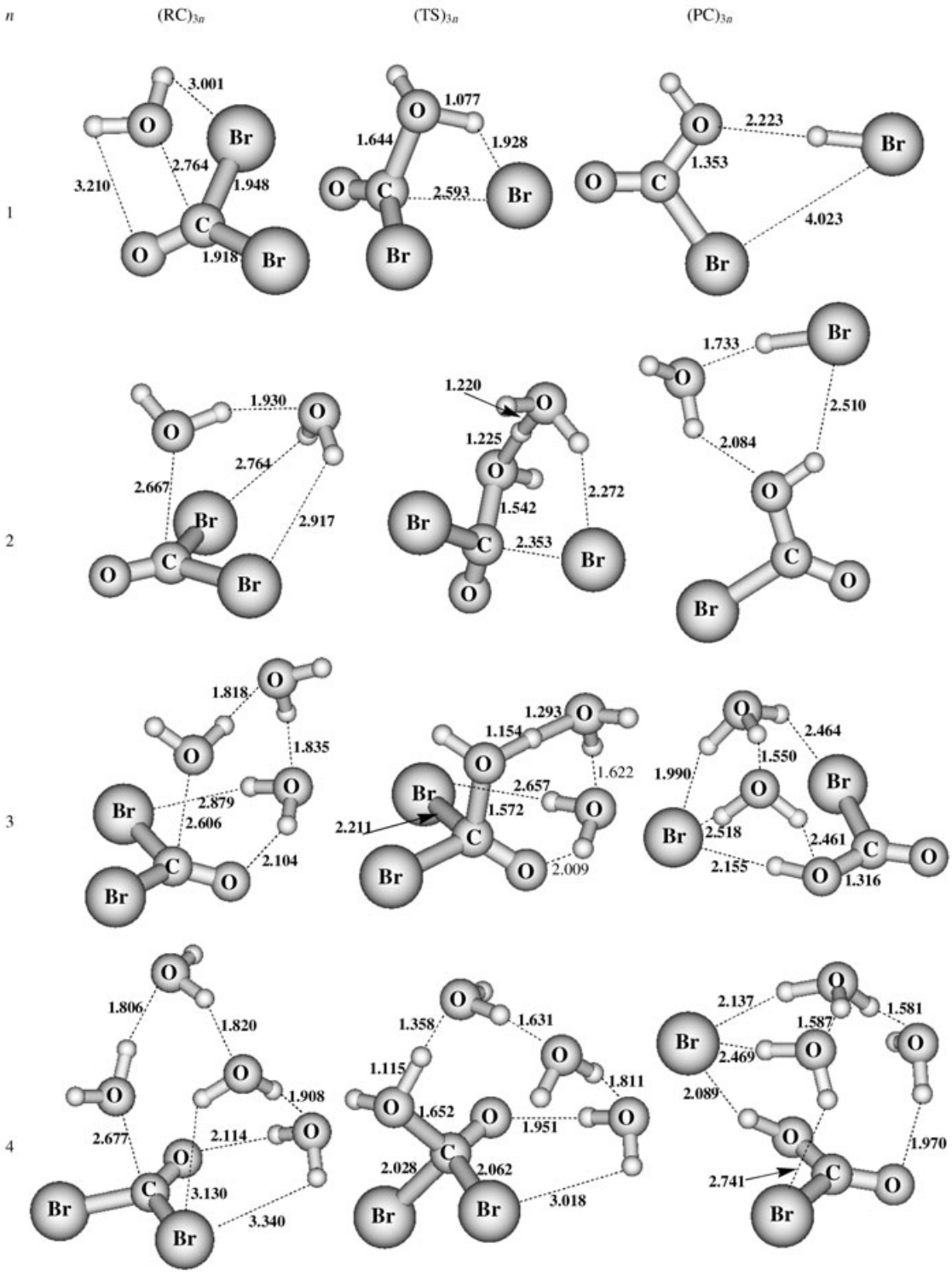

Figure 7. Optimized geometries for the reactant complexes, transition states, and product complexes obtained from MP2/6-31G* calculations for the $CBr_2O + n\,H_2O \rightarrow BrCOOH + HBr + (n-1)\,H_2O$ ($n = 1, 2, 3, 4$) reactions with $(RC)_{3n}$, $(TS)_{3n}$, and $(PC)_{3n}$, where $n = 1, 2, 3, 4$, respectively.

cules involved in the reaction system increases. This indicates that water assists or catalyzes these reactions. The reaction barrier decreases dramatically from about 15.1 kcal mol^{-1} for $n = 1$ to 1.9 kcal mol^{-1} for $n = 3$ for reaction (1) (Figure 11a), from 13.8 kcal mol^{-1} for $n = 1$ to 0.6 kcal mol^{-1} for $n = 3$ for reaction (2) (Figure 11b), from 30.3 kcal mol^{-1} for $n = 1$ to 10.1 kcal mol^{-1} for $n = 4$ for reaction (3) (Figure 11c), from 45.8 kcal mol^{-1} for $n = 1$ to 22.5 kcal mol^{-1} for

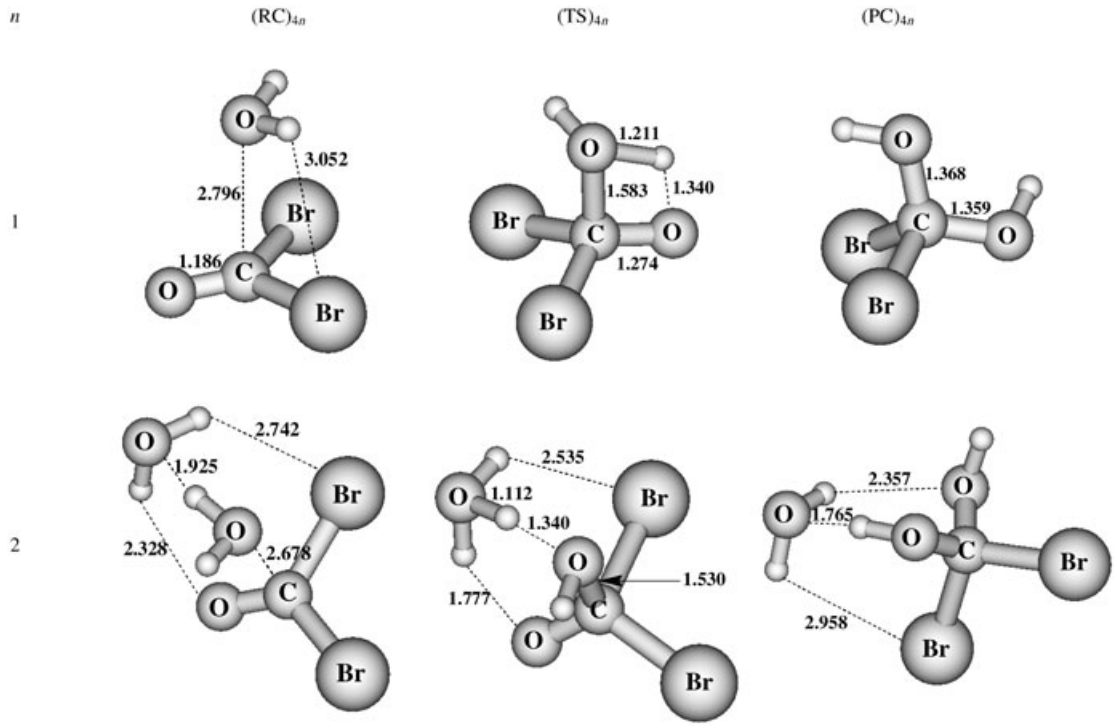

Figure 8. Optimized geometries for the reactant complexes, transition states, and product complexes obtained from MP2/6-31G* calculations for the $CBr_2O + n\,H_2O \rightarrow CBr_2(OH)_2 + (n-1)H_2O$ ($n=1$, 2) reactions with $(RC)_{4n}$, $(TS)_{4n}$, and $(PC)_{4n}$ where $n=1$, 2, respectively.

$n=2$ for reaction (4) (Figure 11 d), from 9.8 kcal mol^{-1} for $n=1$ to 0.2 kcal mol^{-1} for $n=3$ for reaction (5) (Figure 11 e), and from 6.9 kcal mol^{-1} for $n=1$ to 1.2 kcal mol^{-1} for $n=2$ for reaction (6) (Figure 11 f).

It is useful to compare the present ab initio results to those previously found for the dissociation of HBr in H_2O complexes.[35–38] The stabilization energies of the $HBr(H_2O)_n$ clusters changed from 4.2 kcal mol^{-1} for $n=1$ to 54.7 kcal mol^{-1} for $n=5$,[37] and this trend is similar to that found for $X^-(H_2O)_n$ clusters[39,40] and the results found here for isotetrabromomethane$(H_2O)_n$, $CBr_3OH(H_2O)_n$, $CBr_2O(H_2O)_n$, $CBr_2(OH)_2(H_2O)_n$, and $BrCOOH(H_2O)_n$ reactant complexes and transition states. The reactions that involve elimination of an HBr leaving group are similar to the dissociation of HBr in $HBr(H_2O)_n$ clusters. For example, the structures for the product complexes (PC) from the $CBr_3OH(H_2O)_n$ reactions shows that $(PC)_{20}$, $(PC)_{21}$, and $(PC)_{22}$ with $n=0$, 1, 2, respectively, have H···Br distances of 1.437, 1.475, and 1.504 Å, respectively, that are close to the values of 1.4–1.5 Å for a undissociated HBr molecule in $HBr(H_2O)_n$ complexes with $n=0$, 1, 2.[37] Product complex $(PC)_{23}$ from the $[CBr_3OH](H_2O)_n$ reactions has H···Br distances of 1.928 and 2.323 Å that are close to the values of about 2.2 Å for a dissociated HBr molecule in $HBr(H_2O)_n$ complexes with $n=4$, 5.[37] This suggests that HBr is mostly dissociated in the $[CBr_3OH](H_2O)_3$ product complex $(PC)_{23}$. Similar behavior was found in most of the other reactions that produce an HBr leaving group. For example, for the $CBr_2O(H_2O)_n$ reactions $(PC)_{31}$ and $(PC)_{32}$ have H···Br distances of 1.438 and 1.482 Å, respectively, consistent with undissociated HBr, which change to 2.089 and 2.137 Å in $(PC)_{34}$ with $n=4$, consistent with a with almost complete dissociation of HBr into H_3O^+ and Br^-.[37] These results for the reactions that involve an HBr leaving group indicate that addition of more water molecules leads to greater stabilization, lower reaction barriers from reactant complexes to their respective transition state, and greater dissociation of the HBr leaving group in the product complexes.

An NBO analysis was done to estimate the charge on the Br leaving group for the reactant complexes, transition states, and product complexes examined in Figure 5–10 (Table 1).

The charges on the leaving Br atom in the product complexes $(PC)_{11}$, $(PC)_{12}$, $(PC)_{13}$, $(PC)_{20}$, $(PC)_{21}$, $(PC)_{22}$, $(PC)_{31}$, $(PC)_{32}$, $(PC)_{50}$, $(PC)_{51}$, $(PC)_{60}$, and $(PC)_{61}$ range from −0.22 to −0.37. However, the NBO charges increase substantially to the −0.629 to −0.76 range for product complexes like $(PC)_{23}$, $(PC)_{33}$, $(PC)_{34}$, $(PC)_{52}$, $(PC)_{53}$ and $(PC)_{62}$ that have more water molecules for the corresponding reaction systems. This is consistent with the $(PC)_{11}$, $(PC)_{12}$, $(PC)_{13}$, $(PC)_{20}$, $(PC)_{21}$, $(PC)_{22}$, $(PC)_{31}$, $(PC)_{32}$, $(PC)_{50}$, $(PC)_{51}$, $(PC)_{60}$, and $(PC)_{61}$ complexes having Br–H distances in the range of 1.4–1.5 Å for a undissociated HBr molecule.[37] However, the $(PC)_{23}$, $(PC)_{33}$, $(PC)_{34}$, $(PC)_{52}$, $(PC)_{53}$, and $(PC)_{62}$ complexes have longer H–Br distances in the range of 1.8–2.3 Å for a partially to completely dissociated HBr molecule.[37]

The terminal Br atom of isotetrabromomethane has NBO charges of −0.58, −0.49, and −0.67 for $(RC)_{11}$, $(RC)_{12}$, and

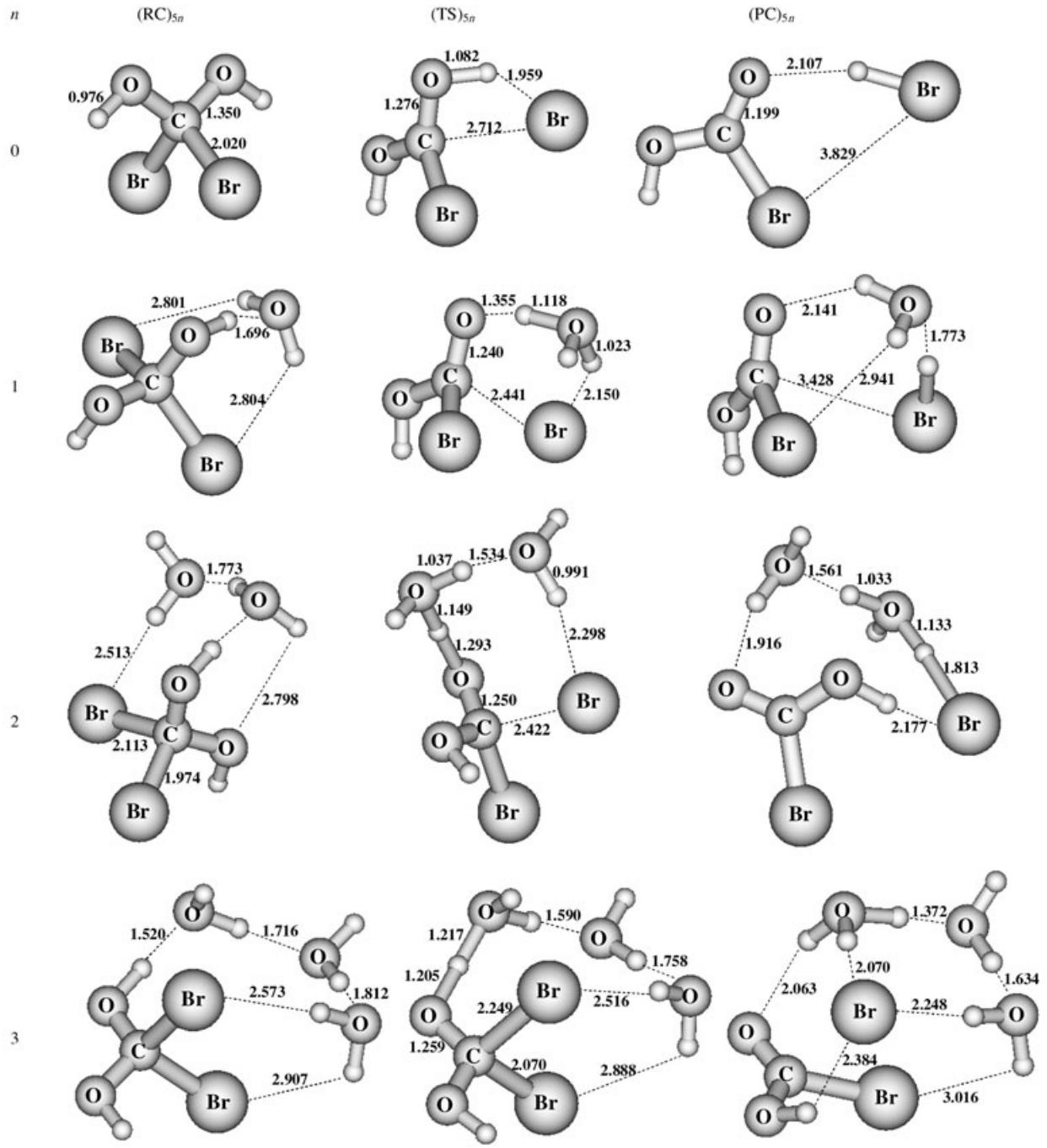

Figure 9. Optimized geometries for the reactant complexes, transition states, and product complexes obtained from MP2/6-31G* calculations for the $CBr_2(OH)_2 + n\,H_2O \rightarrow BrCOOH + HBr + n\,H_2O$ ($n = 0, 1, 2, 3$) reactions with $(RC)_{5n}$, $(TS)_{5n}$, and $(PC)_{5n}$, where $n = 0, 1, 2, 3$, respectively.

$(RC)_{13}$, respectively, for reaction 1. These charges are consistent with isotetrabromomethane having $Br_2C{-}Br^{+}\cdots Br^{-}$ character, similar to isobromoform and other isopolyhalomethane molecules.[29] The charge on the terminal Br atom increases as the RC approaches its respective transition state and has values of −0.803 for $(TS)_{11}$, −0.832 for $(TS)_{12}$, and −0.803 for $(TS)_{13}$. The NBO charges initially on the Br leaving group of the reactant complexes are smaller for the other reactions examined, consistent with these systems having more covalent character than the isotetrabromomethane reactant complexes. For reactions 2, 3, 5, and 6, the charges on the Br leaving group increase substantially on going from their reactant complexes to the corresponding transition states, and as the number of water molecules increases there tends to be less change in the negative charge of the Br leaving group as the reaction goes from its reactant complex to its transition state. For example, the charge changes by −0.597 from $(RC)_{31}$ to $(TS)_{31}$, by −0.503 from

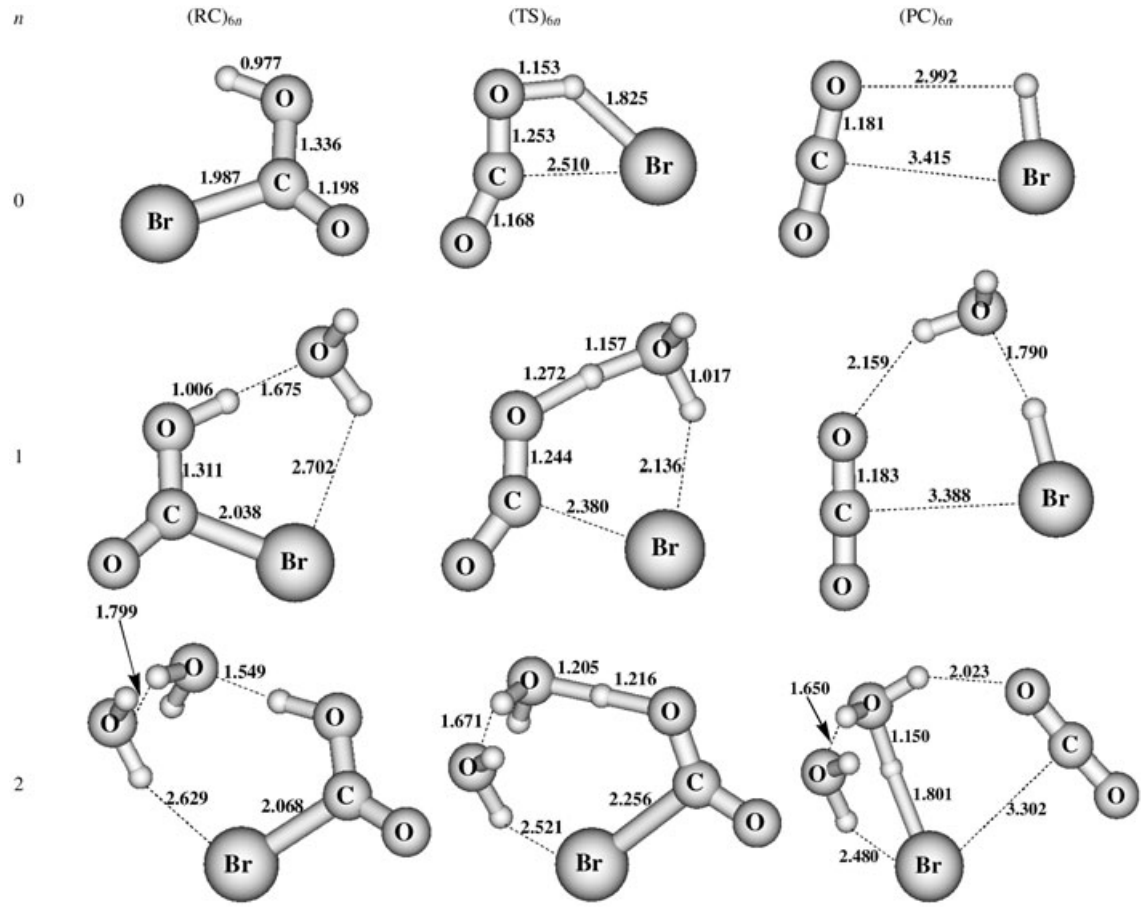

Figure 10. Optimized geometries for the reactant complexes, transition states, and product complexes obtained from MP2/6-31G* calculations for the $BrCOOH + n H_2O \rightarrow CO_2 + HBr + n H_2O$ ($n = 0, 1, 2$) reactions with $(RC)_{6n}$, $(TS)_{6n}$, and $(PC)_{6n}$, where $n = 0, 1, 2$, respectively.

Table 1. NBO charges on the leaving Br atom for the reactant complexes, transition states, and product complexes investigated in Figures 5–10 that have an HBr leaving group.

Reactant complex	Transition state	Product complex	Δ(TS−RC)
$(RC)_{11}$ −0.581	$(TS)_{11}$ −0.803	$(PC)_{11}$ −0.227	−0.222
$(RC)_{12}$ −0.491	$(TS)_{12}$ −0.832	$(PC)_{12}$ −0.242	−0.341
$(RC)_{13}$ −0.671	$(TS)_{13}$ −0.803	$(PC)_{13}$ −0.340	−0.132
$(RC)_{20}$ +0.054	$(TS)_{20}$ −0.490	$(PC)_{20}$ −0.231	−0.543
$(RC)_{21}$ +0.002	$(TS)_{21}$ −0.436	$(PC)_{21}$ −0.312	−0.438
$(RC)_{22}$ −0.027	$(TS)_{22}$ −0.501	$(PC)_{22}$ −0.367	−0.474
$(RC)_{23}$ −0.003	$(TS)_{23}$ −0.027	$(PC)_{23}$ −0.733	−0.024
$(RC)_{31}$ +0.020	$(TS)_{31}$ −0.578	$(PC)_{31}$ −0.227	−0.597
$(RC)_{32}$ +0.020	$(TS)_{32}$ −0.483	$(PC)_{32}$ −0.309	−0.503
$(RC)_{33}$ +0.032	$(TS)_{33}$ −0.332	$(PC)_{33}$ −0.700	−0.364
$(RC)_{34}$ +0.053	$(TS)_{34}$ −0.113	$(PC)_{34}$ −0.742	−0.167
$(RC)_{50}$ −0.048	$(TS)_{50}$ −0.670	$(PC)_{50}$ −0.246	−0.621
$(RC)_{51}$ −0.109	$(TS)_{51}$ −0.542	$(PC)_{51}$ −0.315	−0.434
$(RC)_{52}$ −0.196	$(TS)_{52}$ −0.574	$(PC)_{52}$ −0.629	−0.379
$(RC)_{53}$ −0.199	$(TS)_{53}$ −0.387	$(PC)_{53}$ −0.761	−0.188
$(RC)_{60}$ −0.080	$(TS)_{60}$ −0.507	$(PC)_{60}$ −0.210	−0.427
$(RC)_{61}$ −0.167	$(TS)_{61}$ −0.538	$(PC)_{61}$ −0.304	−0.372
$(RC)_{62}$ −0.214	$(TS)_{62}$ −0.468	$(PC)_{62}$ −0.663	−0.254

$(RC)_{32}$ to $(TS)_{32}$, by −0.364 from $(RC)_{33}$ to $(TS)_{33}$, and by −0.167 from $(RC)_{34}$ to $(TS)_{34}$. Similar trends are also found for the other reactions that have an HBr leaving group. The smaller changes in the charge distribution on the leaving Br atom as the number of water molecules increases suggests less energy is required for redistribution of the charge to the leaving group as the reaction goes from the reactant complex to its transition state. This appears to correlate with generally smaller structural changes taking place (see Figures 5–10), lower reaction barrier heights (e.g., from reactant complex to transition state), and a more highly dissociated

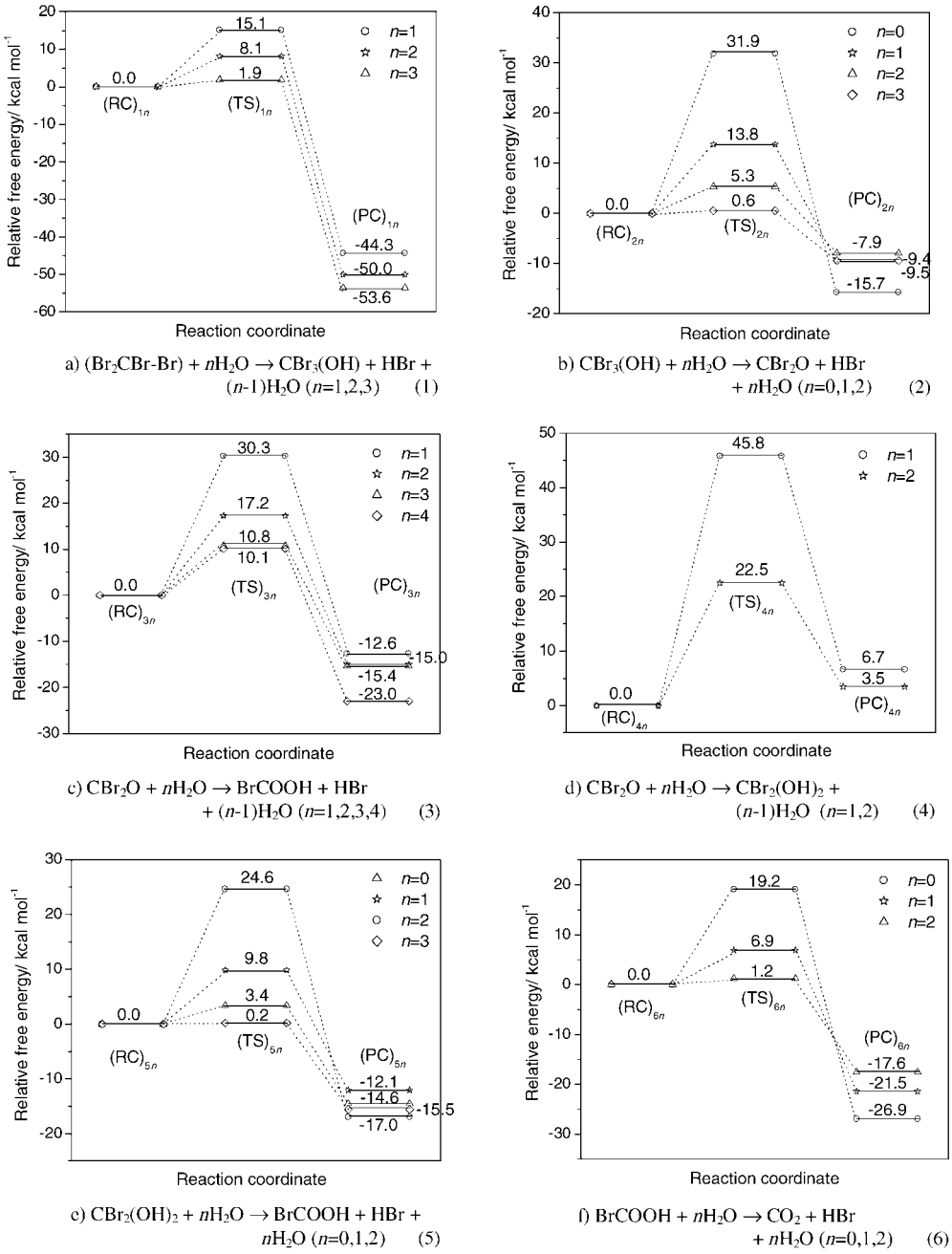

a) $(Br_2CBr\text{-}Br) + nH_2O \rightarrow CBr_3(OH) + HBr + (n\text{-}1)H_2O$ (n=1,2,3) (1)

b) $CBr_3(OH) + nH_2O \rightarrow CBr_2O + HBr + nH_2O$ (n=0,1,2) (2)

c) $CBr_2O + nH_2O \rightarrow BrCOOH + HBr + (n\text{-}1)H_2O$ (n=1,2,3,4) (3)

d) $CBr_2O + nH_2O \rightarrow CBr_2(OH)_2 + (n\text{-}1)H_2O$ (n=1,2) (4)

e) $CBr_2(OH)_2 + nH_2O \rightarrow BrCOOH + HBr + nH_2O$ (n=0,1,2) (5)

f) $BrCOOH + nH_2O \rightarrow CO_2 + HBr + nH_2O$ (n=0,1,2) (6)

Figure 11. Relative free energy profiles (298.15 K, in kcal mol^{-1}) obtained from MP2/6-31G* ab initio calculations on the reactions shown in a)–f). The optimized stationary structures associated the above reactions are shown in Figures 5–10.

character of the HBr molecule in the product complexes as the number of H_2O molecules increases in these reactions. These trends are consistent with water catalysis of the reactions having a HBr leaving group and with solvation and dissociation of the HBr leaving group helping to drive these reactions.

Discussion

Mechanism for the overall major decomposition reaction $CBr_4 + h\nu + n(H_2O) \rightarrow CO_2 + 4HBr + (n-2)H_2O$: On the basis of the present experimental and theoretical results in conjunction with literature data, the following reaction mechanism is proposed for the overall major decomposition reaction $CBr_4 + h\nu + n(H_2O) \rightarrow CO_2 + 4HBr + (n-2)H_2O$ observed after photolysis of low concentrations of CBr_4 in aqueous solution:

Step 1: Photolysis of CBr_4 to produce CBr_3 and Br fragments:

$$CBr_4 + h\nu \rightarrow CBr_3 + Br$$

Step 2: Solvent-induced geminate recombination of the CBr_3 and Br fragments to produce isotetrabromomethane:

$$CBr_3 + Br \rightarrow \text{isotetrabromomethane}$$

Step 3: Water-catalyzed O–H insertion/HBr elimination of isotetrabromomethane with $n\,H_2O$:

$$\text{isotetrabromomethane} + n\,H_2O \rightarrow CBr_3OH + HBr + (n-1)\,H_2O$$

Step 4: Water-catalyzed HBr elimination of CBr_3OH with $n\,H_2O$:

$$CBr_3OH + (n-1)\,H_2O \rightarrow CBr_2O + HBr + (n-1)\,H_2O$$

Step 5: Water-catalyzed hydroysis of CBr_2O and HBr elimination:

$$CBr_2O + (n-1)\,H_2O \rightarrow BrCOOH + HBr + (n-2)\,H_2O$$

Step 6: Water-catalyzed HBr elimination of BrCOOH:

$$BrCOOH + (n-2)\,H_2O \rightarrow CO_2 + HBr + (n-2)\,H_2O$$

Overall reaction: Adding steps 1–6 gives the overall reaction for the major product:

$$CBr_4 + h\nu + n\,H_2O \rightarrow CO_2 + 4\,HBr + (n-2)\,H_2O$$

The CBr_2O intermediate can also be converted to BrCOOH by a two-reaction process:

Step 7a: O–H insertion:

$$CBr_2O + (n-1)\,H_2O \rightarrow CBr_2(OH)_2 + (n-2)\,H_2O$$

Step 7b: HBr elimination:

$$CBr_2(OH)_2 + (n-2)\,H_2O \rightarrow BrCOOH + HBr + (n-2)\,H_2O$$

This two-step process may be in competition with step 5 in the proposed reaction mechanism. Since the barrier for the O–H insertion of step 7a is larger than the barrier for step 5, we expect that the two-step process is of minor importance compared to step 5.

Ultraviolet photolysis at wavelengths longer than 250 nm for many polyhalomethanes containing bromine and/or iodine in the gas and solution phases typically leads to direct cleavage of a carbon–halogen bond to produce haloalkyl radical and halogen atom fragments. This suggests that step 1 in the proposed reaction mechanism is the primary photochemical beginning of the CBr_4 photodissociation reaction. The Ps-TR[3] experiments indicate that some of the initially formed CBr_3 and Br fragments undergo solvent-induced geminate recombination to produce appreciable amounts of the isotetrabromomethane intermediate (see Figure 3), similar to isopolyhalomethane formation after UV photolysis of a range of other polyhalomethanes at room temperature in solution.[28–30,33,34,41–47] This demonstrates that step 2 of the proposed reaction mechanism occurs. The decay of the isotetrabromomethane intermediate becomes much faster with increasing amounts of water in the solvent system (see Figures 3 and 4), and this suggests that isotetrabromomethane reacts with water. This observation, coupled with the ab initio results which show that isotetrabromomethane can readily undergo an O–H insertion/HBr elimination reaction with water to form CBr_3OH + HBr products and the recent direct ps-TR[3] observation of an analogous reaction for the closely related isobromoform (isobromoform $+ n\,H_2O \rightarrow CHBr_2OH + HBr + (n-1)\,H_2O$)[28,29], provides strong support for step 3 of the proposed reaction mechanism for the decomposition of CBr_4 in water.

The ab initio results given here indicate that CBr_3OH can undergo water-assisted HBr elimination to produce CBr_2O + HBr products, similar to previous ab initio studies that showed that halomethanols undergo water-catalyzed HX elimination reactions to produce the corresponding (halo)formaldehyde.[29,30] Other halomethanols such as $CHCl_2OH$ were experimentally observed to decompose into HClCO + HCl in the gas phase and to decompose much faster in aqueous solutions, consistent with water-assisted decomposition of halomethanols.[48–50] The closely related CCl_3OH was found to decompose into CCl_2O + HCl.[48] These experimental results are consistent with our present ab initio results for the water-assisted decomposition of CBr_3OH into CBr_2O + HBr and provide additional support for step 4 of our proposed reaction mechanism for decomposition of CBr_4 after photolysis in water.

Previously reported ab initio calculations for the reaction of CBr_2O with H_2O predicted overall formation of CO_2 + 2 HBr via two potential reaction steps similar to steps 5 and 6 and steps 7a and 7b, but the barriers to reaction were found to be relatively high.[51] Our present ab initio calculations on these reactions agree with these previous results and show that explicit involvement of additional H_2O molecules in the reaction system substantially lowers the barrier heights for the reaction steps that involve elimination of HBr and likely efficient formation of CO_2 + 2 HBr from decomposition of CBr_2O in a water-solvated environment. We note that the closely related CCl_2O molecule was found to decompose into CO_2 + 2 HCl in aqueous solution,[52] consistent with our present ab initio results for reaction of CBr_2O with water. The ab initio results for CBr_2O reacting with water and the experimentally observed decomposition of CCl_2O to produce CO_2 + 2 HCl provide additional support for steps 5 and 6 in our proposed mechanism. The proposed reaction mechanism helps explain how UV photolysis of CBr_4 at low concentration in water leads to formation of the CO_2 and 4 HBr products observed in our photochemical ex-

periments. The reaction mechanism is also consistent with a range of experimental and theoretical results in the literature for the individual reaction steps, for example, the known photolysis of polyhalomethanes into haloalkyl radical and X atom fragments, solvent-induced geminate recombination of these fragments into appreciable amounts of the very reactive isopolyhalomethane species, O–H insertion reactions of isopolyhalomethanes with water, decomposition of halomethanols into (halo)formaldehydes and HX, the predicted decomposition reaction of CBr_2O, and the known decomposition of CCl_2O.

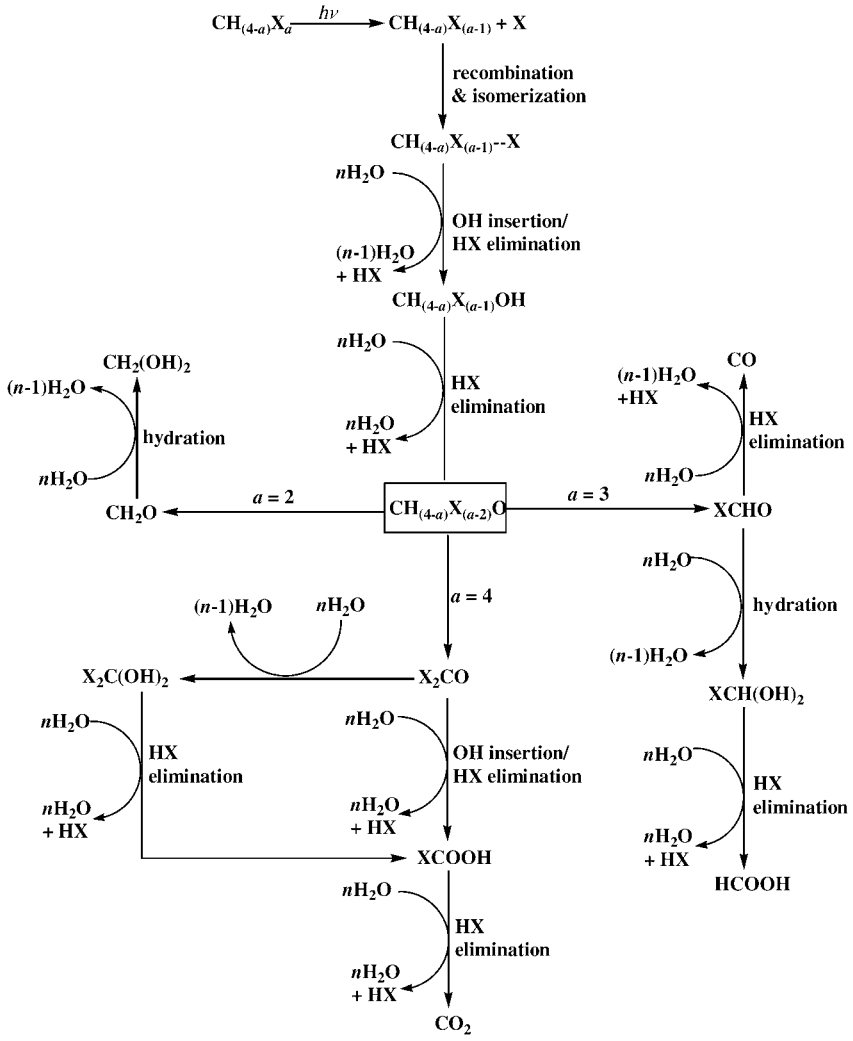

Scheme 1. Proposed general reaction scheme for the UV photolysis of di-, tri-, and tetrahalomethanes ($CH_{4-a}X_a$, where $a = 2$, 3, 4, and X = Cl, Br, I).

General reaction scheme for UV photolysis of dihalo-, trihalo-, and tetrahalomethanes at low concentration in water-solvated environments: why the products associated with the carbon atom are different: Comparison of our present results for the UV photolysis of CBr_4 (a typical tetrahalomethane) in water with previous studies on dihalomethanes (CH_2I_2)[30] and trihalomethanes ($CHBr_3$)[28,29,62] enables us to deduce a general reaction scheme for the UV photolysis of polyhalomethanes at low concentration in water-solvated environments.

Scheme 1 presents this scheme and reveals that the first few reaction steps are common to dihalo-, trihalo-, and tetrahalomethanes. Initial carbon–halogen bond cleavage in step 1, solvent-induced geminate recombination of the haloalkyl radical and halogen atom fragments to form appreciable amounts of isopolyhalomethane in step 2, the isopolyhalomethane O–H insertion/HX elimination reaction with water to produce a halomethanol product and HX leaving group in step 3, and the water-assisted halomethanol HX elimination reaction to produce a (halo)formaldehyde product and HX leaving group in step 4 are very similar for all of the polyhalomethanes studied so far.[28–30,62] The first four steps of the reaction mechanism account for the release of the first two HX leaving groups. The fate of the (halo)formaldehyde is the key step that determines what kind of final carbon products are produced. For dihalomethanes such as CH_2I_2, a formaldehyde product is produced, and it undergoes the known hydrolysis reaction with water to produce the methanediol product (step 5a for dihalomethanes) observed experimentally in photochemical experiments.[30] For trihalomethanes such as $CHBr_3$, a haloformaldehyde product is formed and mostly undergoes water-catalyzed HX elimination to produce the CO product (step 5b for trihalomethanes) experimentally observed in photochemical experiments.[28,29] The haloformaldehyde product can also decompose via a minor reaction pathway by which a hydrolysis reaction with water first forms halomethanediol product ($HXC(OH)_2$) that then decays by a water-assisted HX elimination reaction to produce the HCOOH product (steps 5c and 6a for trihalomethanes) observed experimentally in photochemical experiments.[29] For tetrahalomethanes such as CBr_4, examined in the present study, the dihaloformaldehyde (CX_2O) mainly decomposes by water-catalyzed hydrolysis/HX elimination to first produce XCOOH and a HX leaving group and a water-catalyzed HX elimination reaction of XCOOH to form another HX leaving group and the CO_2 product (steps 5d and 6b, respectively) observed experimentally in photochemical experiments (see Figure 2). The

general reaction scheme shown in Scheme 1 helps explain why UV photolyses of dihalomethanes such as CH_2I_2 in water produce a methanediol final product from the carbon atom, whereas trihalomethanes such as $CHBr_3$ produce mostly CO and some HCOOH, and tetrahalomethanes produce mostly CO_2 from the carbon atom of the polyhalomethane. The general reaction scheme is also consistent with a range of experimental and theoretical results in the literature for the photolysis of polyhalomethanes in aqueous environments and the known decomposition reactions of halomethanols and haloformaldehydes.

Implications for the decomposition of polyhalomethanes, halomethanols, and haloformaldehydes in water-solvated environments: Ultraviolet excitation of most polyhalomethanes with wavelengths longer than 250 nm results in mostly direct carbon–halogen bond cleavage to produce haloalkyl radical and halogen atom fragments with a near-unity quantum yield. However, in aqueous solution several polyhalomethanes containing Br and/or I (CH_2I_2, $CHBr_3$, and CBr_4) have been observed to produce multiple strong acid leaving groups and various carbon-atom products depending on how many halogen atoms are present in the polyhalomethane. This indicates that the photochemistry of polyhalomethanes has significant phase dependence, that is, very different reactions occur in water-solvated environments and the gas phase. We note that a number of isopolyhalomethanes have been experimentally observed after photolysis of polyhalomethanes (containing I, Br, and/or Cl) in condensed-phase environments.[28–30,33,41–47,53–61] This and the observation of isopolyhalomethanes in largely aqueous solutions[30,33] suggest their water-solvated chemistry may be applicable to many different polyhalomethanes. The water-catalyzed reactions of isopolyhalomethanes and their subsequent products are potentially important sources of halogens and/or acid formation in the natural environment and, to our knowledge, have not been considered in the water-solvated photochemistry of polyhalomethanes (CH_2I_2, CH_2BrI, CH_2Br_2, $CHBr_3$, CCl_4, CCl_3F, and others) that have been observed in the environment from natural and/or anthropogenic sources.[1–11]

Ultraviolet photolysis of low concentrations of polyhalomethanes in water-solvated environments releases varying amounts of strong acid HX, depending on the number of halogen atoms that are present in the polyhalomethane. Dihalomethanes release 2 HX, trihalomethanes release 3 HX, and tetrahalomethanes release 4 HX, as shown in Scheme 1. Thus, the more halogens in the polyhalomethane, the more HX groups polyhalomethane photolysis in aqueous environments can release. In addition, the di-, tri-, and tetrahalomethanes produce distinctly different products associated with the carbon atom ($CH_2(OH)_2$ from dihalomethanes such as CH_2I_2, mostly CO with some HCOOH from trihalomethanes such as $CHBr_3$, and mostly CO_2 from tetrahalomethanes such as CBr_4). These different carbon-atom products may be useful markers to help elucidate which polyhalomethanes contribute to water-solvated photochemistry of polyhalomethanes under different environmental conditions.

A number of reactions in the natural environment depend on pH, and these include halogen activation reactions, which are currently attracting intense interest.[12–22] Reactions like $HOX+H^++X^-\rightarrow X_2+H_2O$ (X = Cl and/or Br) and/or $HOX^-+H^+\rightarrow X+H_2O$ have been proposed as the significant activation step in which H^+ and X^- help activate the halogen atom on aqueous particles of sea salt.[12–22] One could reasonably speculate that UV photolysis of polyhalomethanes in water-solvated environments could release noticeable amounts of HX that would in turn affect the pH and possibly influence these types of halogen activation processes. However, more work is needed to elucidate how the water-solvated photochemistry of polyhalomethanes may possibly influence the release of halogens in the natural environment, particularly for acid catalyzed reactions in heterogeneous and/or multiphase environments. We anticipate that this will become an active area of research.

Halogenated methanols such as bromomethanol and chloromethanol can be produced in the atmosphere by reaction of hydroxymethyl radicals with atomic or molecular halogens in the gas phase and can possibly act as a halogen reservoir in the atmosphere.[1] Chloromethanol was experimentally observed to have a lifetime of at least 100 s (and probably longer) for homogeneous decomposition in the gas phase and to decay into HCl and H_2CO.[48,49] The decay of chloromethanol was found to be much faster on surfaces.[48,49] Similarly, dichloromethanol and trichloromethanol were found to decay into HClCO + HCl and CCl_2O + HCl, respectively, in the gas phase and to decay much faster in aqueous solutions.[48] This, combined with our present ab initio computational results for the decomposition of CBr_3OH and previous work on decomposition of $CHBr_2OH$ and CH_2IOH as a function of the number of water molecules present, indicates that the decomposition of halomethanols will be greatly accelerated by water, and their decomposition would probably mostly occur by reactions in water-solvated environments such as water clusters and/or interfacial and/or bulk regions of water/ice particles rather than by homogeneous decomposition. We note that O–H insertion reactions of isopolyhalomethanes with water provide a new and convenient photochemical route to produce halogenated methanols that could be utilized to explore the chemistry of these compounds in condensed phases.

The water-assisted decomposition of trihalomethanes and tetrahalomethanes produces halogenated formaldehydes HXCO and X_2CO, respectively. The HXCO species has been observed to decay mostly to CO + HX in the gas phase and decays much faster in aqueous solution,[50] consistent with the water-catalyzed reaction deduced from ab initio calculations for the $CHBrO+nH_2O\rightarrow CO+HBr+nH_2O$ reaction. The decomposition of X_2CO species, such as Br_2CO examined here, proceeds via two water-catalyzed steps with HBr leaving groups to decay to CO_2 + 2 HBr in the presence of water. The ab initio studies for the decomposition of BrHCO and Br_2CO in water suggests that de-

composition of these halogenated formaldehydes will be greatly accelerated by the presence of water. Thus, decay via this route may be important in the natural environment, although more work is needed to directly assess whether this is actually the case.

Conclusion

Ultraviolet photolysis of low concentrations of CBr_4 in water leads to mostly formation of four HBr leaving groups and CO_2. Ps-TR^3 experiments and ab initio computational results indicate that the water-catalyzed O–H insertion/HBr elimination reaction of isotetrabromomethane and subsequent reactions of its products leads to formation of the 4 HBr and CO_2 products, and a reaction mechanism was proposed. The UV photolyses of di-, tri-, and tetrahalomethanes at low concentrations in water-solvated environments were compared to each other, and a general reaction scheme was elucidated that can account for their different products. The first four steps of the reaction mechanism account for the release of the first two HX leaving groups for the di-, tri-, and tetra-halomethanes. The further reactions of the (halo)formaldehydes are the key steps that determine what type of final carbon-atom products are formed and the total number of HX groups released by dehalogenation of the polyhalomethane. Dihalomethanes such as CH_2I_2 form a formaldehyde product that undergoes the known hydrolysis reaction with water to produce the methanediol product observed experimentally in photochemical experiments and can release two HX leaving groups.[30] Trihalomethanes such as $CHBr_3$ form a haloformaldehyde product that then undergoes mostly a water-catalyzed HX elimination reaction to produce the CO product experimentally observed in photochemical experiments and can release three HX groups.[28,29] The present study on a typical tetrahalomethane (CBr_4) indicates that a dihaloformaldehyde (CX_2O) is produced and then mainly decomposes by water-catalyzed hydrolysis/HX elimination to first produce XCOOH and a HX leaving group and a water-catalyzed HX elimination reaction of XCOOH to form another HX leaving group and the CO_2 product observed experimentally in photochemical experiments (see Figure 2); tetrahalomethanes can release a total of four HX groups. The probable implications for the decomposition of polyhalomethanes, halogenated methanols, and halogenated formaldehydes in water-solvated environments and possibly in the natural environment were briefly discussed. The decomposition of polyhalomethanes, halogenated methanols, and halogenated formaldehydes in water-solvated environments is expected to be greatly accelerated by the presence of water molecules and to exhibit significant differences to their gas-phase decomposition.

Acknowledgement

This research has been supported by grants from the Research Grants Council of Hong Kong (HKU/7036/04P) and (HKU 1/01C) to D.L.P. W.M.K. would like to thank the University of Hong Kong for a Postdoctoral Fellowship.

[1] R. P. Wayne, *Chemistry of Atmospheres*, 3rd ed., Oxford University Press, Oxford, **2000**.
[2] M. J. Molina, F. S. Rowland, *Nature* **1974**, *249*, 810–812.
[3] M. J. Molina, T. L. Tso, L. T. Molina, F. C.-Y. Wang, *Science* **1987**, *238*, 1253–1257.
[4] Th. Class, K. Ballschmiter, *J. Atmos. Chem.* **1988**, *6*, 35–46.
[5] S. Klick, K. Abrahamsson, *J. Geophys. Res.* **1992**, *97*, 12683–12687.
[6] K. G. Heumann, *Anal. Chim. Acta* **1993**, *283*, 230–245.
[7] R. M. Moore, M. Webb, R. Tokarczyk, R. Wever, *J. Geophys. Res. [Oceans]* **1996**, *101*, No. C9, 20899–20908.
[8] C. T. McElroy, C. A. McLinden, J. C. McConnell, *Nature* **1999**, *397*, 338–341.
[9] J. C. Mössonger, D. E. Shallcross, R. A. Cox, *J. Chem. Soc. Faraday Trans.* **1998**, *94*, 1391–1396.
[10] L. J. Carpenter, W. T. Sturges, S. A. Penkett, P. S. Liss, *J. Geophys. Res. [Atmos.]* **1999**, *104*, 1679–1689.
[11] B. Alicke, K. Hebestreit, J. Stutz, U. Platt, *Nature* **1999**, *397*, 572–573.
[12] S. M. Fan, D. J. Jacob, *Nature* **1992**, *359*, 522–524.
[13] M. Mozurkewich, *J. Geophys. Res. [Atmos.]* **1995**, *100*, D7, 14199–14207.
[14] R. Vogt, P. J. Crutzen, R. Sander, *Nature* **1996**, *383*, 327–333.
[15] R. Sander, P. J. Crutzen, *J. Geophys. Res. [Atmos.]* **1996**, *101*, D4, 9121–9138.
[16] K. W. Oum, M. J. Lakin, D. O. DeHaan, T. Brauers, B. J. Finalyson-Pitts, *Science* **1998**, *279*, 74–77.
[17] C. T. McElroy, C. A. McLinden, J. C. Connell, *Nature* **1999**, *397*, 338–341.
[18] R. Vogt, R. Sander, R. V. Glasow, P. J. Crutzen, *J. Atmos. Chem.* **1999**, *32*, 375–395.
[19] W. Behnke, M. Elend, U. Krüger, C. Zetzsch, *J. Atmos. Chem.* **1999**, *34*, 87–99.
[20] E. M. Knipping, M. J. Lakin, K. L. Foster, P. Jungwirth, D. J. Tobias, R. B. Gerber, D. Dabdub, B. J. Finalyson-Pitts, *Science* **2000**, *288*, 301–306.
[21] B. J. Finalyson-Pitts, J. C. Hemminger, *J. Phys. Chem. A* **2000**, *104*, 11463–11477.
[22] K. L. Foster, R. A. Plastridge, J. W. Bottenheim, P. B. Shepson, B. J. Finalyson-Pitts, C. W. Spicer, *Science* **2001**, *291*, 471–474.
[23] C. D. O'Dowd, J. L. Jimenez, R. Bahreini, R. C. Plagan, J. H. Seinfeld, K. Hamerl, L. Pirjola, M. Kulmala, S. G. Jennings, T. Hoffmann, *Nature* **2002**, *417*, 632–636.
[24] I. Nicole, J. de Laat, M. Dore, J. P. Duguet, H. Suty, *Environ. Technol.* **1991**, *12*, 21–31.
[25] O. Legrini, E. Oliveros, A. M. Braun, *Chem. Rev.* **1993**, *93*, 671–698.
[26] C. von Sonntag, G. Mark, R. Mertens, M. N. Schuchmann, H. P. Schuchmann, *Aqua (Oxford)* **1993**, 42, 201–211.
[27] P. Dowideit, C. von Sonntag, *GWF Wasser/Abwasser* **1996**, 137, 268.
[28] W. M. Kwok, C. Y. Zhao, Y.-L. Li, X. Guan, D. L. Phillips, *J. Chem. Phys.* **2004**, *120*, 3323–3332.
[29] W. M. Kwok, C. Y. Zhao, Y.-L. Li, X. Guan, D. Wang, D. L. Phillips, *J. Am. Chem. Soc.* **2004**, *126*, 3119–3131.
[30] W. M. Kwok, C. Y. Zhao, X. Guan, Y.-L. Li, Y. Du, D. L. Phillips, *J. Chem. Phys.* **2004**, *120*, 9017–9032.
[31] Gaussian 98 (Revision 5.4), M. J. Frisch, G. W. Trucks, H. B. Schlegel, G. E. Scuseria, M. A. Robb, J. R. Cheeseman, V. G. Zakrzewski, J. A. Montgomery Jr., R. E. Stratmann, J. C. Burant, S. Dapprich, J. M. Millam, A. D. Daniels, K. N. Kudin, M. C. Strain, O. Farkas, J. Tomasi, V. Barone, M. Cossi, R. Cammi, B. Mennucci, C. Pomelli, C.; Adamo, S. Clifford, J. Ochterski, G. A. Petersson, P. Y. Ayala, Q. Cui, K. Morokuma, D. K. Malick, A. D. Rabuck, K. Raghavachari,

J. B. Foresman, J. Cioslowski, J. V. Ortiz, A. G. Baboul, B. B. Stefanov, G. Liu, A. Liashenko, P. Piskorz, I. Komaromi, R. Gomperts, R. L. Martin, D. J. Fox, T. Keith, M. A. Al-Laham, C. Y. Peng, A. Nanayakkara, C. Gonzalez, M. Challacombe, P. M. W. Gill, B. Johnson, W. Chen, M. W. Wong, J. L. Andres, C. Gonzalez, M. Head-Gordon, E. S. Replogle, J. A. Pople, J. A. Gaussian, Inc., Pittsburgh, PA, **1998**.

[32] a) C. Gonzalez, H. B. Schlegel, *J. Chem. Phys.* **1989**, *90*, 2154–2161; b) C. Gonzalez, H. B. Schlegel, *J. Phys. Chem.* **1990**, *94*, 5523–5527.

[33] W. M. Kwok, C. Ma, A. W. Parker, D. Phillips, M. Towrie, P. Matousek, D. L. Phillips, *J. Phys. Chem. A* **2003**, *107*, 2624–2628.

[34] X. Zheng, W.-H. Fang, D. L. Phillips, *J. Chem. Phys.* **2000**, *113*, 10934–10946.

[35] C. Conley, F. M. Tao, *Chem. Phys. Lett.* **1999**, *301*, 29–36.

[36] B. J. Gertner, G. H. Peslherbe, J. T. Hynes, *Isr. J. Chem.* **1999**, *39*, 273–281.

[37] E. M. Cabaleiro-Lago, J. M. Hermida-Ramón, J. Rodríguez-Otero, *J. Chem. Phys.* **2002**, *117*, 3160–3168.

[38] S. M. Hurley, T. E. Dermota, D. P. Hydutsky, A. W. Castleman, Jr., *Science* **2002**, *298*, 202–204.

[39] H. M. Lee, K. S. Kim, *J. Chem. Phys.* **2001**, *114*, 4461–4471.

[40] M. Kowal, R. W. Gora, S. Roszak, J. Lexzczynski, *J. Chem. Phys.* **2001**, *115*, 9260–9265.

[41] A. N. Tarnovsky, J.-L. Alverez, A. P. Yartsev, V. Sündstrom, E. Åkesson, *Chem. Phys. Lett.* **1999**, *312*, 121–130.

[42] A. N. Tarnovsky, M. Wall, M. Gustafson, N. Lascoux, V. Sündstrom, E. Åkesson, *J. Phys. Chem. A* **2002**, *106*, 5999–6005.

[43] M. Wall, A. N. Tarnovsky, T. Pascher, V. Sündstrom, E. Åkesson, *J. Phys. Chem. A* **2003**, *107*, 211–217.

[44] A. N. Tarnovsky, V. Sündstrom, E. Åkesson, T. Pascher, *J. Phys. Chem. A* **2004**, *108*, 237.

[45] W. M. Kwok, C. Ma, A. W. Parker, D. Phillips, M. Towrie, P. Matousek, D. L. Phillips, *J. Chem. Phys.* **2000**, *113*, 7471–7478.

[46] W. M. Kwok, C. Ma, A. W. Parker, D. Phillips, M. Towrie, P. Matousek, X. Zheng, D. L. Phillips, *J. Chem. Phys.* **2001**, *114*, 7536–7543.

[47] W. M. Kwok, C. Ma, A. W. Parker, D. Phillips, M. Towrie, P. Matousek, D. L. Phillips, *Chem. Phys. Lett.* **2001**, *341*, 292–298.

[48] T. J. Wallington, W. F. Schneider, I. Barnes, K. H. Becker, J. Sehested, O. J. Nielsen, *Chem. Phys. Lett.* **2000**, *322*, 97–102.

[49] G. S. Tyndall, T. J. Wallington, M. D. Hurley, W. F. Schneider, *J. Phys. Chem.* **1993**, *97*, 1576–1582.

[50] P. Dowidiet, R. Mertens, C. von Sonntag, *J. Am. Chem. Soc.* **1996**, *118*, 11288–11292.

[51] J. S. Francisco, *Chem. Phys. Lett.* **2002**, *363*, 275–282.

[52] R. Mertens, C. von Sonntag, *Angew. Chem.* **1994**, *106*, 1320–1322; *Angew. Chem. Int. Ed. Engl.* **1994**, *33*, 1259–1261.

[53] G. Maier, H. P. Reisenauer, *Angew. Chem.* **1986**, *98*, 829–831; *Angew. Chem. Int. Ed. Engl.* **1986**, *25*, 819–822.

[54] G. Maier, H. P. Reisenauer, J. Hu, L. J. Schaad, B. A. Hess, Jr., *J. Am. Chem. Soc.* **1990**, *112*, 5117–5122.

[55] X. Zheng, D. L. Phillips, *Chem. Phys. Lett.* **2000**, *324*, 175-.

[56] X. Zheng, D. L. Phillips, *J. Phys. Chem. A* **2000**, *104*, 6880–6886.

[57] X. Zheng, D. L. Phillips, *J. Chem. Phys.* **2000**, *113*, 3194.

[58] X. Zheng, C. W. Lee, Y.-L. Li, W.-H. Fang, D. L. Phillips, *J. Chem. Phys.* **2001**, *114*, 8347–8356.

[59] Y.-L. Li, K. H. Leung, D. L. Phillips, *J. Phys. Chem. A* **2001**, *105*, 10621–10625.

[60] Y.-L. Li, D. M. Chen, D. Wang, D. L. Phillips, *J. Org. Chem.* **2002**, *67*, 4228–4235.

[61] Y.-L. Li, D. Wang, D. L. Phillips, *J. Chem. Phys.* **2002**, *117*, 7931–7941.

[62] C. Y. Zhao, D. Q. Wang, D. L. Phillips, *J. Chem. Phys.*, submitted.

Received: July 8, 2004
Published online: December 22, 2004